



HAL
open science

Absolute Temperature Measurement on tungsten surfaces with monochrome and bicolor IR thermography

D Guilhem, Y Corre, X Courtois, J Gaspar, C Pocheau, S Vives

► To cite this version:

D Guilhem, Y Corre, X Courtois, J Gaspar, C Pocheau, et al.. Absolute Temperature Measurement on tungsten surfaces with monochrome and bicolor IR thermography. Nuclear Fusion, In press, 10.1088/1741-4326/ac0e73 . hal-03579912

HAL Id: hal-03579912

<https://amu.hal.science/hal-03579912>

Submitted on 18 Feb 2022

HAL is a multi-disciplinary open access archive for the deposit and dissemination of scientific research documents, whether they are published or not. The documents may come from teaching and research institutions in France or abroad, or from public or private research centers.

L'archive ouverte pluridisciplinaire **HAL**, est destinée au dépôt et à la diffusion de documents scientifiques de niveau recherche, publiés ou non, émanant des établissements d'enseignement et de recherche français ou étrangers, des laboratoires publics ou privés.



Distributed under a Creative Commons Attribution - NonCommercial - NoDerivatives 4.0 International License

Absolute Temperature Measurement on tungsten surfaces with monochrome and bicolor IR thermography

D. Guilhem¹, Y. Corre¹, X. Courtois¹, J. Gaspar², C. Pocheau¹, S. Vives¹

¹ CEA, IRFM, F-13108 St Paul lez Durance, France

² Aix Marseille Univ, CNRS, IUSTI, Marseille, France

E-mail: dominique.guilhem@cea.fr

Received xxxxxx

Accepted for publication xxxxxx

Published xxxxxx

Abstract

ITER (<https://www.iter.org>) will take advantage of tungsten (W) actively cooled Plasma Facing Units (PFU) in the lower divertor. These PFUs will receive a steady state plasma heat flux of 10 MW/m² and up to 20 MW/m² in slow transients, pushing these components to their limit. For machine protection reasons and for the study of the plasma wall interactions, temperature measurements are foreseen with Mid Wave Infra-Red (MWIR: 3-5 μm) thermography systems to cover most of ITER chamber including the divertor (tungsten material) and first wall (beryllium material) [1]. Absolute temperature measurements from 70 °C, the cooling temperature of the PFUs, up to 3500 °C (W melting temperature at 3422 °C), are considered. Those measurements require the knowledge of the emissivity of the tungsten PFU surfaces as function of the temperature and wavelength used for the IR monochrome thermography system. This paper summarizes the emissivity measurements performed on tungsten surfaces in High Heat Flux (HHF) test beds and the WEST tokamak [2] and uses the experimental emissivity values to compute the expected uncertainties in ITER ($\Delta T/T$) using monochrome and bicolor thermography techniques. Results show that monochrome technique is not able to fulfill the $\Delta T/T < 10\%$ requirement, while bicolor technique is able to reduce the temperature uncertainty below 10%. Laboratory bicolor thermography measurements using a filter wheel (including 6 MWIR interference filters) have been successfully performed up to 830°C with temperature uncertainty $\Delta T/T < 3\%$. In the WEST tokamak, the two dimensions emissivity map is varying by a factor of five within 27 cm along a PFU, from 0.13 to 0.65, showing that the monochrome IR thermography will have difficulties to stay within the ITER requirements $\Delta T/T < 10\%$ from 70 °C up to 3500 °C.

Keywords: Thermography, Tungsten, Emissivity, Monochrome, Bicolor

1 Introduction

The primary role of the IR thermography systems in fusion devices such as tokamak or stellarator, is absolute surface temperature measurement, roles for which the diagnostic is expected to be well suited for ITER. It falls in the categories: machine protection, basic control, advanced control and finally physics measurements [3]. This diagnostic is expected to make absolute surface temperature measurements (in °C) with relative uncertainty $< 10\%$, as given in the ITER requirements. It is well known [4,5] that the surface temperature measurement of the Plasma Facing Components (PFC) in ITER will be difficult due to highly reflecting materials such as tungsten and beryllium, used for divertor and first wall respectively, having a low and varying emissivity during plasma exposition, evolving with surface state, temperature, wavelength, and angle of observation. One of the

other main challenges is the physical environment in which all these measurements have to be done. These are: the transmission evolution of the thermography system, thermal properties of the targets, first mirror degradation due to plasma deposition/erosion, specular reflection on the observed object from others hot spots in the machine, multiples reflections from the “sphere effect” (hot divertor radiating in a highly reflective environment), bremsstrahlung emission from the plasma, radiation effect on refractive optics (blackening) and camera detector (noise). As it is shown, the surface state of the PFC (deposition/erosion) during plasma operation is the main driving parameter of the local effective emissivity.

The first part of the paper deals with the emissivity of tungsten surfaces reported in HHF tests and tokamak facilities. In WEST, in-situ measurement [6] have recently shown that

emissivity varies significantly along one W-coated graphite PFU. Low emissivities are found in the Inner and Outer Strike Point areas (ISP, OSP) where the power density is high, corresponding to an erosion zone. Higher emissivities are found in the re-deposition areas located away from the plasma strike point footprints. Slow variation of the surface emissivity is observed along the experimental campaign, as the magnetic equilibrium and plasma parameters are always changing during plasma experiments. The second part of the paper deals with monochrome IR thermography and more particularly the uncertainty of the absolute temperature measurement as function of the uncertainty of the emissivity that have been derived from the published literature. The emissivity variations observed in WEST are used to compute the accuracy of the IR monochrome thermography. The third part of the paper deals with bicolor thermography temperature measurement. This technique is not relying on absolute emissivity at one wavelength, but relying on the ratio of the emissivities at two relatively close wavelengths. An experimental set-up has been specifically designed to investigate the temperature uncertainties using six different interference filters in laboratory (up to 850°C).

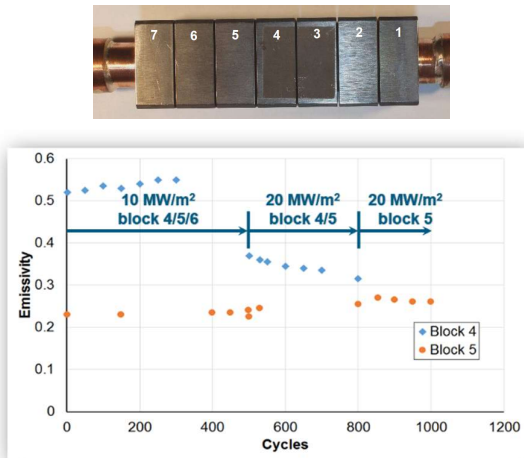


Figure 1. (Top) Image of the 7 monoblocks ITER-like PFU mockup. (Bottom) Emissivity variation of the surface of 2 monoblocks during the screening test [12].

2 Emissivity of tungsten surfaces

Hemispherical total emissivity and spectral emissivity of tungsten has been measured for decades [7,8]. For the last 15 years, a large number of HHF tests have been performed with ITER like PFU mockups made of different grade of tungsten [9], with different techniques (grinding, electro discharge machining), from different material makers, from different manufacturers. Currently, the applicability of the world-wide developed manufacturing technologies of tungsten monoblock plasma facing components has been confirmed by intensive HHF testing, e.g. 5 000 cycles at 10 MW/m² and 1 000 cycles at 20 MW/m², on mock-ups of ITER divertor [9]. It is observed during HHF tests on real monoblocks of PFU mock-ups at GLADIS (10.75 μm) [10] and JUDITH (3.85 μm) [11,12], strong variations of the emissivity, up to a factor 2 figure 1.

Testing was done on Judith-1 of an ITER-like PFU mock-up made of 7 monoblocks, by thermal cycling at 10 MW/m² and 20 MW/m² with a maximum of 1200 cycles at 10 MW/m² followed by 500 cycles at 20 MW/m² without obvious damage formation. The difference of the emissivity between blocks 4 and 5 is due to a preloading of block 4 causing a strong surface roughening and a larger emissivity. At 10 MW/m² during the screening test of figure 1, no degradation of the surfaces is observed. At the very beginning of cycling at 20 MW/m² we see a strong modification of the emissivity of block 4 associated to induced surface modifications caused by local high power density of the beam spot on small W grains, leading to their erosion [12]. At FE200 (3.99 μm) [13], measurement of the emissivity of ITER like PFU tungsten mockup have been done as a function of temperature. Finally, a dedicated campaign was conducted at CEA laboratory in 2018 to measure the emissivity of tungsten samples [14], from 200 to 800 °C for different central wavelengths from 1.7 to 4.75 μm. These samples were cut in a real ITER PFU mockup to ensure a good representability of what is expected in ITER. All these observed emissivities during PFU test campaigns at worldwide facilities, GLADIS, JUDITH, FE-200 and CEA (laboratory), are plotted figure 2. It shows large differences between the different measurements. The difference of the emissivity between the HHF tests is not known since within the publications there is usually no clear indication on the state of the observed samples (Presence of deposition and surface composition prior to the tests, Ra, cracks, etc.). The dashed lines represents the modified extended Hagen-Rubens model (see below).

2.1 Analytical models

The emissivity of pure ideal metallic material (undamaged, no crack, pristine mirror-like surface) has been modelled by expressions: Drude $\varepsilon = \frac{a}{\sqrt{\lambda}}$, Hagen-Rubens $\varepsilon = a \sqrt{\frac{T}{\lambda}}$, exponential $\varepsilon = e^{a\lambda + bT}$, polynomial $\varepsilon = \sum_{k=0}^n a(k) \lambda(k)$, etc. Unfortunately, these models are not adequate to represent the experimental measurement variations of the emissivity with wavelength and temperature. An extension of the Hagen-Rubens model [15] has been proposed [16], which improves the agreement of the model with experiments.

$\varepsilon(\lambda, T)$ increases with temperature increase and decreases with wavelength increase:

$$\varepsilon_{\lambda}(T) = 0.365 \sqrt{\frac{\rho(T)}{\lambda}} - 0.0667 \frac{\rho(T)}{\lambda} + 0.006 \sqrt{\left(\frac{\rho(T)}{\lambda}\right)^3} \quad (1)$$

where $\rho(T) = \rho_0 (1 + \alpha \Delta T)$ is the electrical resistivity at temperature T. The tungsten electrical resistivity at 20 °C $\rho_0 = 5.5 \cdot 10^{-6}$ Ohm-cm, and the coefficient of variation of the electrical resistivity is $\alpha = 5.2 \cdot 10^{-3} \text{ K}^{-1}$.

Figure 2 shows the measured normal emissivity at different HHF test facilities and test stand: JUDITH in the 2-5.7 μm band [17], GLADIS at 10.75 μm [10], FE200 at 3.99 μm [13] and finally at CEA in 2018 at 4.35 μm on a dedicated test

bench. One can see that large differences are apparent, for example at 800°C the data from CEA (4.35 μm) indicates $\varepsilon = 0.143$ and for FE200 (3.99 μm) $\varepsilon = 0.243$. An equation scaling inversely with the square root of the wavelength agrees with the trend of the data [13], which are falling as well with increasing temperature. Note that a slope and an offset have to be added to the extended Hagen-Rubens (HR) emissivity:

$$\varepsilon = \text{Offset} + \text{Slope} \times \text{HR-Emissivity}(\lambda, T).$$

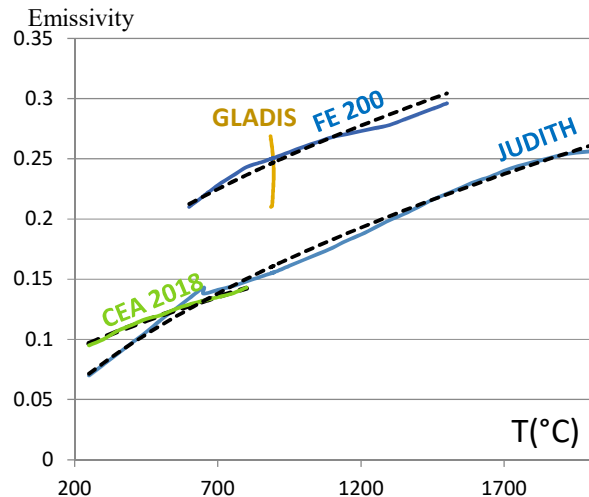


Figure 2. Tungsten emissivity dependence as a function of temperature. These measurements were done during HHF tests at JUDITH (3.85 μm – Lower blue line), GLADIS (10.75 μm – Orange line), FE200 (3.99 μm – Upper blue line), and finally at CEA laboratory (4.35 μm – Green line). Dash lines are the modified extended Hagen-Rubens model, see below.

Figure 2 indicates the results of the modified extended Hagen-Rubens in dash-black lines. The offset and slope are respectively: CEA (0, 1.6), FE200 (0, 2.55), JUDITH (0.11, 2.7). The CEA 2018 experimental measurements on PFU material mockup, have been done in a dedicated, well-controlled and instrumented test-bed.

2.2 Effect of surface state

The emissivity is dependent on the surface state, including oxidation, deposition (especially in tokamaks during machine conditioning or during plasma operation), and surface roughness or eventually due to cracks formation during HHF exposition [14]. It has been observed on real dimensions ITER PFU mockups [18] that the emissivity is strongly dependent on the surface roughness R_a , especially when $R_a < 1.2 \mu\text{m}$. For ITER the PFU specifications indicates $R_a < 1.6 \mu\text{m}$ which is verified on measurements done on six real ITER-like PFU for WEST showing $0.2 < R_a < 1 \mu\text{m}$. In conclusion, the effect of the surface morphology on the emissivity dominates over the temperature and/or wavelength dependences.

2.3 Observations made in WEST during the 2019 experimental campaign

During the WEST 2019 experimental campaign (1523 valid shots with $I_p > 100 \text{ kA}$), some semi-inertial (the PFU is not actively cooled, but its support is actively cooled) graphite PFUs coated with a 10 μm W layer, equipped with embedded

thermocouples were monitored during discharges. The ratcheting effect of the pre-pulse temperature (which increases shot after shot) is completely homogeneous within the PFU. This is exploited to make emissivity profiles along two half PFU equipped with thermocouples. We took advantage of the double heating method assuming that the background radiation is constant prior to the shots [19,6] since most of the plasma facing component supports are actively cooled at 70 °C by a dedicated water-loop. Figure 3 [24] shows the ISP and OSP positions on the two half of one PFU, in the configuration mostly exploited during the experimental campaign. Ten optical lines (endoscope + IR camera) [19] are installed in the upper ports, each covering a portion of 40° of the lower divertor figure 3. The WEST thermographic system [20] is working at 3.9 μm . The spatial resolution vary within the field of view from 2.3 to 5.4 mm/pixel. For 80% of luminance modulation (which corresponds to a measurement error of 10% @1000 °C), the spatial resolution is 5.4 mm (PFU width ~30 mm). Figure 4 presents a picture of the analyzed PFU, together with a profile of the estimated emissivity distribution, unless this profile is reconstructed from two one-half PFU equipped with thermocouples, located at two different toroidal locations in the machine. It shows a large inhomogeneity along the PFUs, due to erosion at the strike point locations, and re-deposition away from the strike points as it is observed in other tokamaks [21]. Figure 5 presents the temperature map between two shots (no plasma). The global emissivity map cannot be estimated from the IR thermography measurements since the individual temperature of each PFUs is not known due to a limited number of available embedded thermocouples. The profile figure 4 reflects probably the history of all the scenarios encountered with different positions of the ISP and OSP. The non-uniformity of the emissivity profile cannot be directly linked with laboratory emissivity measurements made in ideal condition of pure pristine tungsten, where no plasma erosion or redistribution is taking place. In fact, only the lowest emissivity found, $\varepsilon_{\text{min}} = 0.13$, at the maximum heat flux location of the OSP, is representative of laboratory measurements made on pure W samples. We observe figure 5 that the two dimensions apparent temperature map is complex in the toroidal direction, associated to a non-uniform heat flux map due to the WEST toroidal magnetic field ripple. The modulation of the ripple due to the 18 superconducting coils is complex. In this paper the authors want just to point out the fact that the emissivity pattern is complex in the poloidal direction (factor 5 in the emissivity change over 27 cm) but also toroidal directions (ripple effect), and inevitably the monochrome will have difficulties to assess temperature maps since the emissivity also changes over the temperature increase of the PFC during the pulses. In the case of bicolor measurement, the hypothesis of a constant emissivity ratio over the temperature change during plasma operation is assumed. This emissivity ratio is measured pixel by pixel during the baking of the machine. The question that is raised here is: does this assumption is still valid for a WEST-like PFU in an all-metal machine like WEST during plasma operation? So far we do not have the response. On the other hand for the monochrome IR thermography, we know during WEST operation that 1) the emissivity profiles evolve, profiles obtained between 2 plasma discharges when the PFU temperature is homogeneous (from

two temperature method), 2) at one location the emissivity is evolving with temperature (but we do not know this evolution since it depends on the surface composition and the surface state of each observed area corresponding to 1 pixel (pixel dependent). Post mortem studies are being conducted and will be published. Between two discharges (no plasma), each individual PFU temperature is homogeneous as measured by fibre Bragg gratings (uncertainty: ± 1 °C) placed along some PFU. The emissivity pattern (from $\varepsilon = 0.13$ to $\varepsilon = 0.65$; variation = 5 within 27 cm) along one PFU is evolving during plasma operation (different plasma scenarios) and machine conditioning [14]. The following up over experimental campaign of the 2D emissivity map of the tungsten PFUs should give us some indication on how we could eventually handle this observation. The WEST lower divertor was equipped with graphite tiles coated with ~ 10 μm tungsten on top of ~ 3 μm molybdenum. Six of these PFU were coated additionally with a thin Mo interlayer (~ 0.1 μm) and a W cover layer (1-4 μm) as erosion markers. After experimental campaigns these tiles were analyzed [22] by Rutherford Backscattering Spectroscopy (RBS), and by Nuclear reaction Analyses (NRA) to get the amounts of tungsten, boron, carbon and deuterium (depth profiles). Confocal Laser Scanning Microscopy (CLSM) has also been used for measuring the height profile on microscopic length scale. Net erosion above 1 μm is observed in the OSP and ISP areas as can be concluded from RBS combined with results from scanning electron microscopy (SEM) assisted by energy dispersive X-ray spectroscopy (EDX) and focused ion beam (FIB) cutting. Moderate deposition is observed elsewhere while a sharp transition to thick deposition layers up to the order of 10 μm , is observed near the ISP area. From EDX, no further elements in significant amounts are present in the deposited layers besides the expected ones (W, Mo, carbon, boron from boronisations, copper used in heating devices and finally oxygen due to oxidation at the latest by air exposure after the venting of the vacuum vessel) [22].

The conclusion that we can infer from these observations, is that after plasma exposure most of the surface of the divertor is no longer a pure pristine tungsten material, except at the ISP and OSP where the heat flux is large corresponding to erosion zones. Within material deposition zones in tokamaks, it seems difficult to rely on theoretical or laboratory measurements of the W emissivity, to make in-situ absolute monochrome surface temperature measurements. Absolute temperature measurement rely on the knowledge of emissivity, which is evolving with temperature, wavelength and surface state. Usually in present day machine, the emissivity of the PFCs is supposed to be spatially uniform and not dependent on temperature during shots.

3 Bicolor thermography

3.1 Principle

Another method to measure the absolute surface temperature of an object is to exploit bicolor thermography. Let us see the bicolor technic where the spectral radiance ($\text{W} \cdot \text{sr}^{-1} \cdot \text{m}^{-2} \cdot \text{m}^{-1}$) is measured at two different wavelengths λ_1 and λ_2 . The spectral radiance at the two wavelengths is given by the Planck law:

$$L_i(\varepsilon_i, \lambda_i, T) = \frac{\varepsilon_i C_1 \lambda_i^{-5}}{e^{(C_2/\lambda_i T)} - 1} = f_{\lambda_i}(\varepsilon_i, T) \quad i = 1 \text{ or } 2 \quad (2)$$

When integrated over the Full Width Half Middle (FWHM) of the interference filter of the camera, the result is the irradiance or the power per unit area. We assume for the simplicity of the presentation that the irradiance is proportional to the spectral irradiance since the FWHM of the interferences filters used are generally quite small, $\Delta\lambda = \text{FWHM} \sim 0.2$ μm in our case. On such a small bandwidth, the transmission of the interference filters and spectral irradiances at the two wavelengths are assumed constant. The temperature T measured by the camera is calculated from the measured power flux $P(\lambda, T)$:

$$P(T) = \int_{\lambda} L(\lambda, T) d\lambda \sim L(\lambda, T) \Delta\lambda \quad (3)$$

Assuming the same $\Delta\lambda = \text{FWHM}$ for the interference filters, taking equation (3) at two wavelengths λ_1 and λ_2 , we have three unknowns: ε_1 , ε_2 and T. A system of two equations with three unknowns is undetermined since there is an infinite set of three parameters that fulfill the system. We can reduce these two equations into one equation to calculate the temperature. For wavelength ~ 4 μm the Wien approximation ($\exp(C_2/\lambda T) \gg 1$) is valid up to ~ 500 °C ($\lambda \cdot T < 3124$ $\mu\text{m} \cdot \text{K}$ corresponding to 1% error).

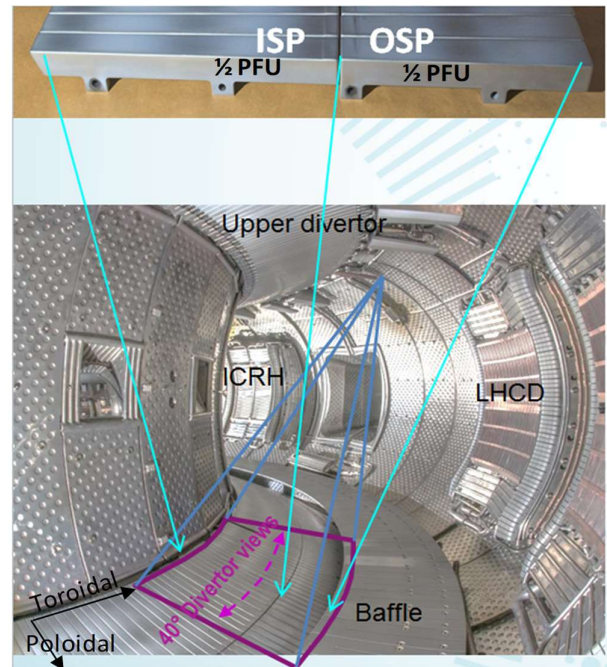


Figure 3. (Top) picture of the two parts of plasma facing units made of graphite coated with a layer of 10 μm of tungsten. (Down) Inside view of WEST tokamak equipped with tungsten covered coated tiles.

When the Wien approximation is valid, we can infer the temperature from:

$$T = \frac{C_2 \left(\frac{1}{\lambda_2} - \frac{1}{\lambda_1} \right)}{\ln \left(\frac{\varepsilon_2}{\varepsilon_1} \frac{L_1}{L_2} \left(\frac{\lambda_2}{\lambda_1} \right)^{-5} \right)} \quad (4)$$

When the Wien approximation is no longer valid, it can be shown that the temperature is calculated from the relation:

$$\underbrace{\frac{\text{Exp}\left(\frac{C_2}{\lambda_2 T_2}\right)-1}{\text{Exp}\left(\frac{C_2}{\lambda_1 T_1}\right)-1}}_{\text{Measured apparent temperatures}} = \varepsilon_R \underbrace{\frac{\text{Exp}\left(\frac{C_2}{\lambda_2 T}\right)-1}{\text{Exp}\left(\frac{C_2}{\lambda_1 T}\right)-1}}_{\text{Look Up Table (LUT)}} = f_{\lambda_1 \lambda_2 \varepsilon_R}(T) \quad (5)$$

where T_1 and T_2 are the apparent temperatures ($\varepsilon = 1$) and $\varepsilon_R = \varepsilon_1 / \varepsilon_2$ the emissivity ratio at λ_1 and λ_2 . The look-up table is only dependent on the emissivities ratio ε_R and the temperature T . The emissivity ratio is calculated from equation (5) during calibration, thanks to known temperature of the divertor (350 °C for ITER), and apparent temperatures T_1 and T_2 measured by the bicolor IR camera. Using the extended Hagen-Rubens emissivity for tungsten [15] we calculated that for the couple of wavelengths $\lambda_1 = 4.4 \mu\text{m}$ and $\lambda_2 = 4.7 \mu\text{m}$, the uncertainty of the relative emissivity ratio is $\Delta\varepsilon_R/\varepsilon_R = 0.15 \%$ for temperatures from 100 °C to 3000 °C. ε_R is measured during calibration, and then assumed constant since its variation with temperature is quite small figure 8.

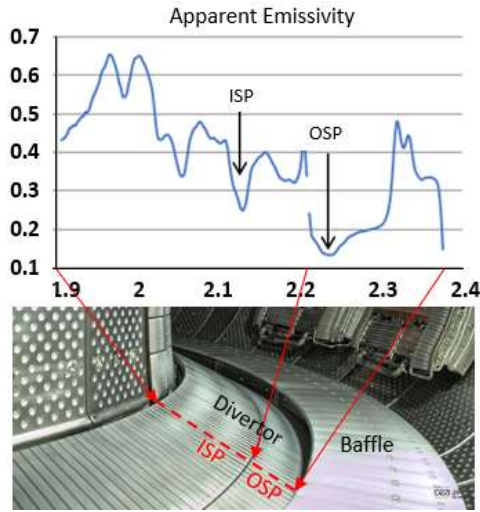


Figure 4. (Up) Measured emissivity profile plotted along a PFU (dash red line) similar to the one showed here. The emissivity varies along the PFU by a factor of ~ 5 within 27 cm, from 0.13 to 0.65. (Down) Picture of divertor equipped with W-coated graphite PFUs.

Figure 5 is the apparent surface temperature map ($\varepsilon = 1$) of one sector of the divertor prior to shot #55946 (-1s). We can observe a strong toroidal and poloidal inhomogeneity of the apparent surface temperatures. Each individual PFU temperature is homogeneous as measured by some thermocouples (uncertainty: $\pm 0.4\%$ of the measure) placed along some PFUs. Figure 5 (bottom) presents the plots of the

thermocouple temperature of a PFU during shots #55945, #55946 and #55963. It evidences the ratcheting effect (increase) of the PFU temperature prior to the shots (-1 s): 115 °C, 161 °C and 204 °C.

We took advantage of shots #55946 and #55963 to calculate the apparent emissivity of the W coated PFU, assuming that the reflected ambient radiance was the same prior to shots.

3.2 Relative temperature uncertainty

The question we can raise about the bicolor technic is the temperature uncertainty dependence, $\Delta T/T$, with the dependence of the uncertainty of the ratio of the emissivities at the two wavelengths. Using the Wien approximation for simplicity of the literal expression, the relative temperature uncertainty considering no error on photons fluxes and wavelength $\partial L/L = \partial \lambda/\lambda = 0$ is:

$$\frac{\Delta T}{T} = \frac{\lambda_R T}{C_2} \frac{\Delta \varepsilon_R}{\varepsilon_R} \quad (7)$$

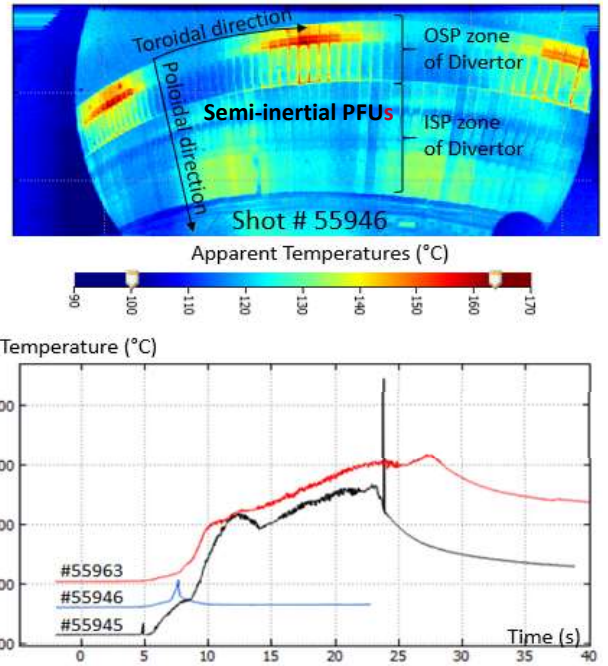


Figure 5. (Top) Apparent ($\varepsilon = 1$) surface temperature of a sector of the divertor (refers to figure 3 for the view). (Bottom). Plot of one PFU thermocouple temperature during shots #55945, # 55946 and #55963.

$$\text{where: } \lambda_R = \frac{\lambda_1 \cdot \lambda_2}{\lambda_2 - \lambda_1} \quad \text{and} \quad \varepsilon_R = \frac{\varepsilon_1}{\varepsilon_2} \quad (8)$$

In the Wien approximation, the relative temperature uncertainty is linearly proportional to the relative emissivities ratio uncertainty. This is not the case at high temperature ($T > 500 \text{ °C}$ at $4 \mu\text{m}$), where it increases more rapidly. Figure 6 presents the uncertainty of the temperature $\Delta T/T$ as a function of the uncertainty of the ratio of emissivities at the two

considered wavelengths, $\lambda_1 = 4.1 \mu\text{m}$ and $\lambda_2 = 4.4 \mu\text{m}$ ($\lambda_R = 69$), without the Wien approximation. For this set of wavelengths we estimated that W emissivity ratio uncertainty $< 0.92\%$ is required to have a temperature uncertainty $< 10\%$ up to $3500 \text{ }^\circ\text{C}$, and $< 1.5\%$ for temperatures up to $1000 \text{ }^\circ\text{C}$. The temperature precision is $\pm 2\%$ for the MWIR camera and 0.4% for type K thermocouple.

3.3 Test of the bicolor technic

We propose to exploit these observations for the bicolor thermography within the MWIR infrared region, measurements made in the CEA laboratory. The test bed was optimized to minimize the effect of any reflected flux from the surrounding, so that residual reflected flux was negligible. We took advantage of a TELOPS® infrared camera fitted with a filter wheel equipped with 6 interference filters: $\lambda_8 = 3.2 \mu\text{m}$ (FWHM = $0.6 \mu\text{m}$), $\lambda_7 = 3.7 \mu\text{m}$ (FWHM = $0.64 \mu\text{m}$), $\lambda_6 = 3.8 \mu\text{m}$ (FWHM = $0.55 \mu\text{m}$), $\lambda_5 = 3.9 \mu\text{m}$ (FWHM = $0.52 \mu\text{m}$), $\lambda_4 = 4.4 \mu\text{m}$ (FWHM = $0.18 \mu\text{m}$) and $\lambda_3 = 4.7 \mu\text{m}$ (FWHM = $0.24 \mu\text{m}$). The tungsten sample was equipped with a K-type thermocouple used as a reference temperature. The reference emissivities and reference emissivity ratio were estimated at the ITER divertor baking temperature of $350 \text{ }^\circ\text{C}$, and then kept constant during the experiment. Figure 7 is a trace of the uncertainty of the measured monochrome temperature at the different wavelengths and of the bicolor temperature, as function of the reference temperature. We estimated that the maximum temperature uncertainty is $15.9\% < \Delta T/T < 23.5\%$ at $850 \text{ }^\circ\text{C}$ for the monochrome technic at different wavelengths (W emissivity measured during calibration at $350 \text{ }^\circ\text{C}$ and then kept fixed), and $\Delta T/T < 3.5\%$ at $822 \text{ }^\circ\text{C}$ for the bicolor technic (W emissivity ratio measured during calibration at $350 \text{ }^\circ\text{C}$ and then kept fixed). The camera accuracy is $\pm 2\%$ as shown figure 7. The bicolor technic matches the thermocouple measurement within the ITER specification.

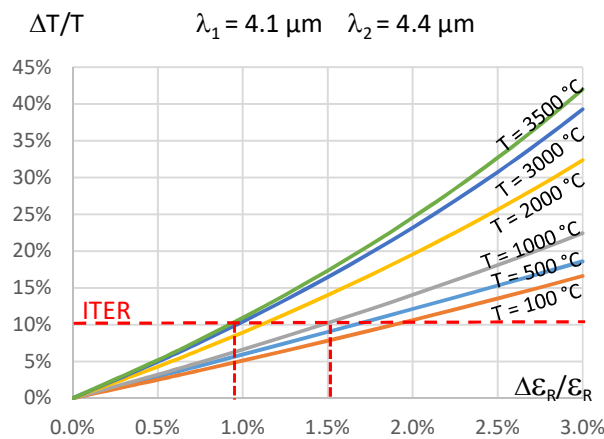


Figure 6. Dependence of the temperature uncertainty $\Delta T/T$ as a function of the relative emissivity uncertainty $\Delta \epsilon_R/\epsilon_R$ for different surface temperatures up to $3500 \text{ }^\circ\text{C}$. The ITER requirement is $\Delta T/T < 10\%$.

The advantage of the bicolor technic is to exploit the ratio of the emissivities at two wavelengths, which is weakly dependent on the temperature at the considered wavelengths. In our experiment the ratio of the emissivities estimated at $350 \text{ }^\circ\text{C}$ was kept constant $\epsilon_R = 0.9402$ to infer the bicolor temperature uncertainty dependence of figure 7. From the measured apparent surface temperatures T'_1 , T'_2 and the thermocouple temperature, one can estimate the sample emissivity evolution with temperature for each wavelength. Figure 8 [24] shows the dependence of the emissivities ratio as a function of the thermocouple temperature. It indicates that the uncertainty on the emissivities ratio is within $\pm 0.3\%$ from 300 to $850 \text{ }^\circ\text{C}$, well below the required accuracy of $\pm 1\%$ to have a temperature uncertainty $\Delta T/T < 10\%$ up to $3500 \text{ }^\circ\text{C}$, figure 6.

4 Conclusion

The main variation of the emissivity is principally due to deposition, presence of cracks or cracks networks on the surface, but also with temperature and wavelength. It depends on the location of the observed zone, in a HHF region where erosion is taking place, or far from the strike point location where we observe deposition. In ITER the PFUs will receive heat flux of 10 MW/m^2 (the design value), after a long process of increasing slowly the heat flux on the PFCs to ascertain the operating scenarios, and after having ensured that surface temperature measurements are made within a maximum relative uncertainty of 10% (in $^\circ\text{C}$) to guaranty the protection of the ITER divertor. If the parts were sound, without presence of any deposition or pollution, no modification of the true surface temperature of the tungsten monoblocks would be expected if the emissivity is known with enough precision. However, we know that baking and conditioning (boronisation) of the metallic walls in present day tokamaks is regularly made. We also know that erosion in the HHF zones and deposition in the low heat flux zones takes place, locations depending on the operating scenario. Unexpected incident could take place at any time, as vertical displacement event, as disruption. Each of these effects may jeopardize the knowledge of the absolute emissivity map needed to make a monochrome surface temperature measurement with a good precision ($< 10\%$). The difficulty with the monochrome surface temperature measurement is the temporal and spatial variation of the emissivity of the PFUs surface material over time (long pulses) and plasma scenarios (moving the strike points). The main difference for the ITER-like actively cooled PFU compared to the W coated graphite semi-inertial PFU (studied in the paper), is the amplitude of the variation of the emissivity along a PFU. For the ITER-like PFU a minimal emissivity value of 0.06 is measured at the OSP and a maximum value of 0.9 ($\times 15$) far away from the ISP (instead of 0.13 , 0.65 and $\times 5$ respectively). These data are to be published with details. As the W-coated PFU have been removed from WEST and replaced by ITER-like PFU (spring 2021), we will repeat the procedure after the restart of operation, and compare the changes. However, we do not anticipate to have a clear and predictable emissivity evolution over experimental campaigns since the major player for the absolute value of the effective emissivity rely on the surface

state (erosion/deposition, baking, conditioning, boronisation, experimental scenario, crack formation, etc...). We cannot detangle all these physical effects since we do not have this information. Much more details can be found on the effective emissivity profile along a W coated PFU in [14].

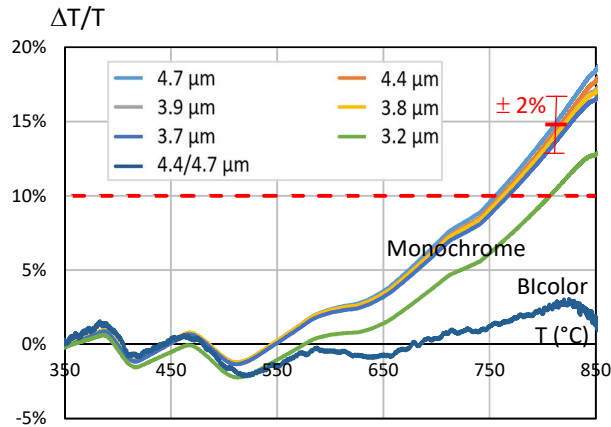


Figure 7. Dependence of the temperature uncertainty (monochrome and bicolor) as a function of the thermocouple temperature (reference). The reference temperature for the emissivities, or ratio of emissivities, is 350°C the baking temperature of the ITER divertor.

It will be valuable in the future to see if the bicolor absolute surface temperature measurement can help to minimize the temperature uncertainty. Concerning the extended Hagen-Rubens emissivity relation, it was experimentally shown that this expression is able to give the tendencies for $\lambda > 2 \mu\text{m}$ for pure pristine mirror-like tungsten, but it is not satisfactory for rough, corroded, oxidized or coated/redeposited surfaces in a real tokamak environment. This particular analytic formulation of the emissivity is not taking into account the diverse surface properties of PFCs, and can be misleading because of the strong variations of the properties of the PFUs surface material during plasma operation over time. Thus, it is not possible to predict the radiative properties of plasma facing components in a tokamak, unless the tungsten surface approach ideal conditions of composition finish and state. This is the case in a well-controlled experiment in a dedicated test bed in a laboratory, but not in a tokamak. The emissivity to apply to each individual pixel of an image (camera frame) is different and dependent on temperature and its time history for each wavelength. One route to get absolute surface temperature is to take advantage of bicolor thermography and have regular calibration of the ratio of the emissivities (and at the same time the transmission of the optical system), pixel-by-pixel during the known baking temperature of the machine (350 °C for the ITER divertor). We have to point out that bicolor thermography has already proved his ability to make good measurements of metallic plasma facing components. This technic has been successfully demonstrated on the NSTX fusion research device [23] where the surface temperature of lithium as it transitioned from solid to liquid and back was observed both when it was electrically heated without the presence of plasma, and when heated by plasma alone, then

cooled by conduction.

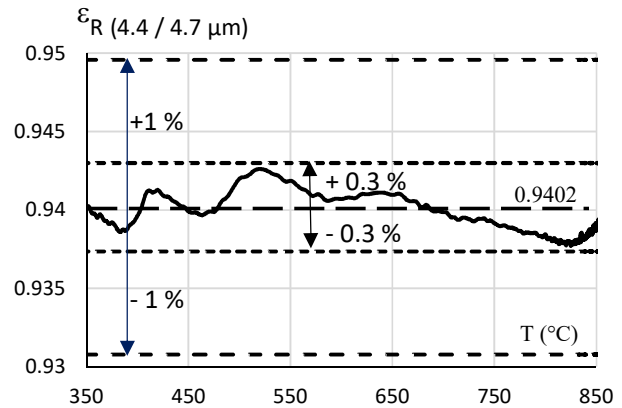


Figure 8. Dependence of the emissivity ratio as a function of the thermocouple reference temperature. The fixed value taken at 350°C for the emissivity ratio is 0.9402 for the bicolor temperature estimation.

References

- [1] Kocan M. et al 2016 Phys. Scr. 2016 014047 <https://iopscience.iop.org/article/10.1088/0031-8949/T167/1/014047>
- [2] Bucalossi J. et al. “The WEST project: Testing ITER divertor high heat flux component technology in a steady state tokamak environment”, Fusion Engineering and Design 89 (2014) 907–912, <https://doi.org/10.1016/j.fusengdes.2014.01.062>
- [3] Reichle R. “System Design Description (DDD) 55.G1 Vis/IR Equatorial Port Wide-Angle Viewing System”; 22 Jan 2015 / 1.4 / Approved; ITER-IDM UID: DCHGAP. Mail to: Roger.Reichle@iter.org
- [4] Guilhem D. et al. “Reflections and surface temperature measurements in experimental fusion reactors Tore-Supra, JET and ITER”; QIRT Journal. Volume 3 – N° 2/2006, pages 155 to 168. <https://doi.org/10.3166/qirt.3.155-168>
- [5] Aumeunier A. et al. « Impact of reflections on the divertor and first wall temperature measurements from the ITER infrared imaging system », Nuclear Materials and Energy (2017). <https://doi.org/10.1016/j.nme.2017.02.014>
- [6] Gaspar J. et al. “In situ assessment of the emissivity of tungsten plasma facing components of the WEST tokamak”, Nuclear Materials and Energy Volume 25, December 2020, 100851 <https://doi.org/10.1016/j.nme.2020.100851>
- [7] Worthing “The true temperature scale of tungsten and its emissive powers at incandescent temperatures”, Phys. Rev. 10, 377 (1917), <https://doi.org/10.1103/PhysRev.10.377>
- [8] Matsumoto T. et al. International, “Hemispherical Total Emissivity of Niobium, Molybdenum, and Tungsten at high Temperatures Using a combined Transient and brief Steady-State Technique”; Journal of Thermophysics, Vol. 20, No 3, 1999. <https://doi.org/10.1023/A:1022699622719>
- [9] Hirai T. et al. “Use of tungsten material for the ITER divertor”, Nuclear Fusion and Energy 9 (2016) 616-622. <https://doi.org/10.1016/j.nme.2016.07.003>
- [10] Greuner H. et al., “High heat flux testing of newly developed tungsten components for WEST”; Task Report HHF-Test of

- M-1-1; Private communication (2015) and SOFT-2016 P4.101. <mailto:henri.greuner@ipp.mpg.de>
- [11] Pintsuk G. “Task report : HHF-Test of M-1-1”, July 2015), Private communication. See “High heat flux testing of newly developed tungsten components for WEST”, SOFT-2016 poster P4.101. <https://indico.ipp.cas.cz/event/4/contributions/1062/>
- [12] High heat flux testing of newly developed tungsten components for WEST, G. Pintsuk (g.pintsuk@fz-juelich.de), et al. To be published in Fusion Engineering and Design)
- [13] Lott F. “Advances in optical thermometry for the ITER divertor” Fusion Engineering and Design 85 (2010) 146-152. <https://doi.org/10.1016/j.fusengdes.2009.08.007>
- [14] Gaspar J. et al., “Emissivity measurement of tungsten plasma facing components of the WEST tokamak”, Fusion Engineering and Design 111328 (2019) 149. <https://doi.org/10.1016/j.fusengdes.2019.111328>
- [15] Hagen E. , Rubens H. “Über die Beziehung des Reflexions- und Emissionsvermögens der Metalle zu ihrem elektrischen Leitvermögen”, Ann. d. Physik, Vol. 4, 11, p 873-901, 1903. Born M., Wolf E., “Principles of Optics”. <https://doi.org/10.1002/andp.19033160811>
- [16] Dmitriev V.D. et al. “Radiant Emissivity of Tungsten in the Infrared Region of the Spectrum”, Zhurnal Prikladnoi Spektroskopii, Vol. 2, No. 6, pp. 481-488, 1965. <https://link.springer.com/content/pdf/10.1007/BF00655100.pdf>
- [17] Richou M. et al. “Realization of high heat flux tungsten monoblock type target with graded interlayer for application to DEMO divertor” M. Phys. Scr. T170 (2017) 014022. <https://doi.org/10.1088/1402-4896/aa8b02>
- [18] Takeushi M. , “Development of the in situ calibration method for ITER divertor thermography”, Fusion Sci. Technol., vol 69, 655-665, May 2016. <https://doi.org/10.13182/FST15-191>
- [19] Walach T. “Emissivity measurements on electronic microcircuits”, Measurement 41 (2008) 503–515. <https://doi.org/10.1016/j.measurement.2007.07.001> <https://doi.org/10.1016/j.nme.2020.100851>
- [20] Courtois X. et al. “Full coverage infrared thermography diagnostic for WEST machine protection”; Fusion Engineering and Design, Volume 146, Part B, 2019, Pages 2015-2020, ISSN 0920-3796. <https://doi.org/10.1016/j.fusengdes.2019.03.090>
- [21] Akola A. et al. “Erosion of tungsten and steel in the main chamber of ASDEX Upgrade” <http://dx.doi.org/10.1016/j.jnucmat.2014.11.034>
- [22] Balden M. et al. “Erosion and redeposition patterns on entire erosion marker tiles after exposure in the first operation phase of WEST”, PFMC 2021, to be published.
- [23] G. McLean “A dual-band adaptor for infrared imaging” -- Rev. Sci. Instrum. 83, 053706 (2012) <https://doi.org/10.1063/1.4717672>
- [24] D. Guilhem et al. “An ITER Challenge Absolute Surface Temperature Measurements of Low and Varying Emissivity Tungsten Plasma-Facing Components”, IEEE TRANSACTIONS ON PLASMA SCIENCE, VOL. 48, NO. 7, JULY 2020 DOI: [10.1109/TPS.2020.2998327](https://doi.org/10.1109/TPS.2020.2998327)